Research Progress in Mechanical and Manufacturing Engineering Vol. 2 No. 2 (2021) 380-389

RPMME

Homepage: http://publisher.uthm.edu.my/periodicals/index.php/rpmme
e-ISSN : 2773-4765

Modelling Numerical Simulation of DP590 Steel Undergoing Finite Strain Deformation of Uniaxial Tensile Test

M. F. Kamarulzaman[1], N. M. Zin[1], M. K. Mohd Nor[1*], M. S. A. Samad[1, 2]

[1]Crashworthiness and Collision Research Group (COLORED)
Mechanical Failure Prevention and Reliability Research Centre (MPROVE)
Faculty of Mechanical and Manufacturing Engineering,
University Tun Hussien Onn Malaysia, MALAYSIA

[2]Computer Aided Engineering, Vehicle Performance, Group Research and Development, Perusahaan Otomobil Nasional Bhd (PROTON), Shah Alam, Selangor, MALAYSIA

*Corresponding Author Designation

DOI: https://doi.org/10.30880/rpmme.2021.02.02.043
Received 20 July 2021; Accepted 25 Nov.2021; Available online 25 Dec. 2021

Abstract: Metal sheets made of Advanced High Strength Steel (AHSS) of Dual Phase (DP) steels are commonly utilised in the automobile industry to form numerous complex forms and sizes of components specifically related to crash energy management. In this paper, the deformation behaviour of DP 590 at various strain rates (0.0001, 0.001, 0.01 and 0.1 s−1) along two principal directions; 0° and 90° are simulated. The tensile behaviour of DP590 was captured in terms of stress-strain curves using the simplified Johnson-Cook (JC) of LS Dyna Finite Element code. The engineering data was first characterised to output the material parameters of JC model which were used further to predict the strain rate dependency of DP590 at various strain rates along the principal directions. A good agreement was obtained in each test.

Keywords: Dual Phase Steel DP590; Finite Strain Deformation; Simplified Johnson-Cook; Numerical Analysis; LS Dyna FE Code

1. Introduction

Steel as a metal is established as one of the most important materials in the present-day scenarios. It has various applications in fields such as aerospace, automotive, infrastructure, and shipbuilding [1]. Nowadays, high strength and low weight advanced structural steels are gaining a special attention in various performance critical applications such as automotive and aerospace sectors [2]. This lead to the extensive development of Advanced High Strength Steels (AHSS) [3].

**Corresponding author: *khir@uthm.edu.my*

DP 590 steel is generally utilised for body panels that are exposed (doors, hoods and fenders). Designers can lower outer panel gauge and weight while preserving or improving dent resistance thanks to its good formability, high work hardening, and bake hardening properties. Because of its application in the automotive industry, extensive study has been done in the past. However, there are few studies that use anisotropic characteristics and ductile fracture criteria to estimate fracture strains at extreme temperatures. As a result, the author attempted to determine the fracture stresses of DP 590 steel at various temperatures by experimentation. The flow behaviour of DP steel has been studied at various strain rates and temperatures. It was predicted using various empirical, or semi-empirical, equations popularly called as constitutive models. The combined effect of strain, temperature, and strain rate over flow stress, for a variety of materials has also analysed in detail by many researchers using various physically and phenomenologically based constitutive models [4].

AHSS, such as DP steel, which is thought to have a more complex deformation behaviour due to its dual phase structure, has been the subject of a few recent studies. As a result, the current study investigates the flow stress behaviour, material characteristics, strain hardening behaviour, and constitutive model development of DP 590 steel at various strain rates. The deformation behaviour of the material can be studied by performing various types of tests like uniaxial tensile, biaxial tensile and compressive tests [5]. Temperature and strain rate effects on the deformation behaviour of DP steels were studied by [6],[7]. They have conducted the tensile tests within the temperature and at strain rates. Finally, they found that the DP steels are insensitive in that temperature range, and sensitive towards strain rates. A microstructure based micromechanical model was developed [8] to capture the deformation behaviour, plastic strain localization and plastic instability of DP 590 steel.

Besides experimental, numerical simulation can also be use. Accurate numerical simulation of tensile test can provide physical insights that cannot be captured by experiments. A constitutive model's complexity is usually proportional to its intended application. Numerical simulations can be used to substitute costly and time-consuming testing, allowing designers to confirm structure reliability and manufacturers to check stated manufacturing procedures before starting production. Generally, constitutive models must have following characteristics: capability to describe important aspects of material behaviour, to be mathematically and computationally simple, and to require a reasonable amount of experimental effort to obtain material parameters [9]. The model's practical value is determined by the difficulty in gathering experimental data and model constants. The creation of relatively easy experimental procedures for characterization of engineering materials for the proposed model is the second major component of this work.

2. Methodology

A numerical analysis was carried out to examine the material model in detail at various strain rate dependent. There are three main steps in an analysis which is geometry development, numerical solution and results interpretation. In LS Pre-Post and LS Dyna software applications, each of these steps corresponds to a different processor. In particular, geometry is created in the pre-processing phase and load operation which is LS-PrePost, and the solution is performed in the Processor phase of the solution known as LS Dyna Manager. Finally, the results are viewed in the general Postprocessor stage. Typical mechanical properties and tensile value of DP590 are listed in Table 1 and Table 2 respectively.

Table 1: Properties of DP 590 steel

Yield strength (MPa)	Tensile strength (MPa)	Total elongation (%)	Young's modulus (GPa)	Poisson's ratio (v)
355-370	620-625	26	185	0.33

Table 2: Tensile value at different strain rates and orientation

Material direction	Strain rate (s^{-1})	Young's modulus (GPa)	Yield stress (MPa)	UTS (MPa)
0°	1×10^{-4}	186.74	346	744
	1×10^{-3}	189.27	355	761
	1×10^{-2}	192.52	364	744
	1×10^{-1}	193.14	371	751
90°	1×10^{-4}	185.39	344	748
	1×10^{-3}	188.28	361	754
	1×10^{-2}	191.10	363	749
	1×10^{-1}	192.69	370	743

2.1 Geometry development

The study was on modelling the material designed to see how the specimen would react at various strain rates. DP 590 steel was used in this project. It is important to keep in mind that the endurance limit (fatigue strength) is related to the tensile strength of the steel. DP steels offer good fatigue characteristics due to their high strength. The tensile strength of DP steels increases with its endurance limit. The specimen's geometry of the uniaxial tensile test was formed according to ASTM E8 dog bone shape specimen standard dimension, as shown in Table 3, which designed specifically for tensile testing. The dog bone shape specimen was modelled using Solidworks software.

Table 3: Standard Geometric of ASTM E8 for Tensile Test's specimen

Parameter	Size (mm)
Gauge length	25.0
Width	6.18
Thickness	1.43
Radius of fillet	6.0
Overall length	100.0
Length of reduced section	32.0
Length of grip section	30.0
Width of grip section	10.0

2.2 Mesh generation

In simulation process, meshing is the factor affecting the accuracy of the result because it organised the arrangement of a discrete point on a model. The existence of different shapes of elements, such as square and triangular, is in order to allow more refined mesh were used for example in areas of high stress concentration where greater accuracy is needed, especially if the shape geometry of model structures is complex. In such cases it is very common to combine square and triangular elements. Also, the number of nodes on each element may also affect the results. There are two types of meshing used in this research which are 2D Mesh and Shape Mesh as shown in Figure 1 and Figure 2 respectively.

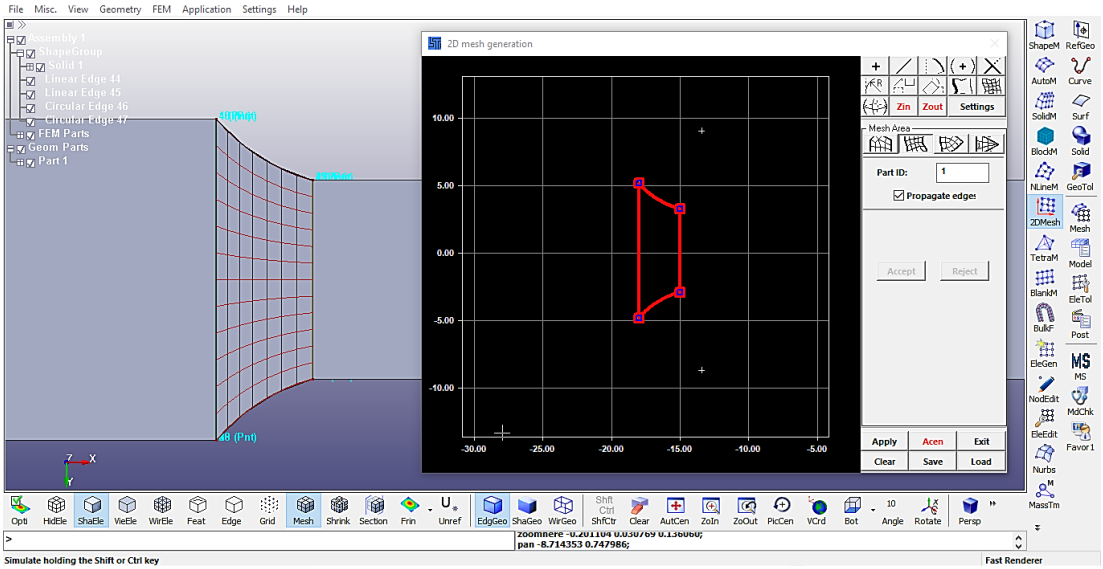

Figure 1: Meshing by using 2D Mesh

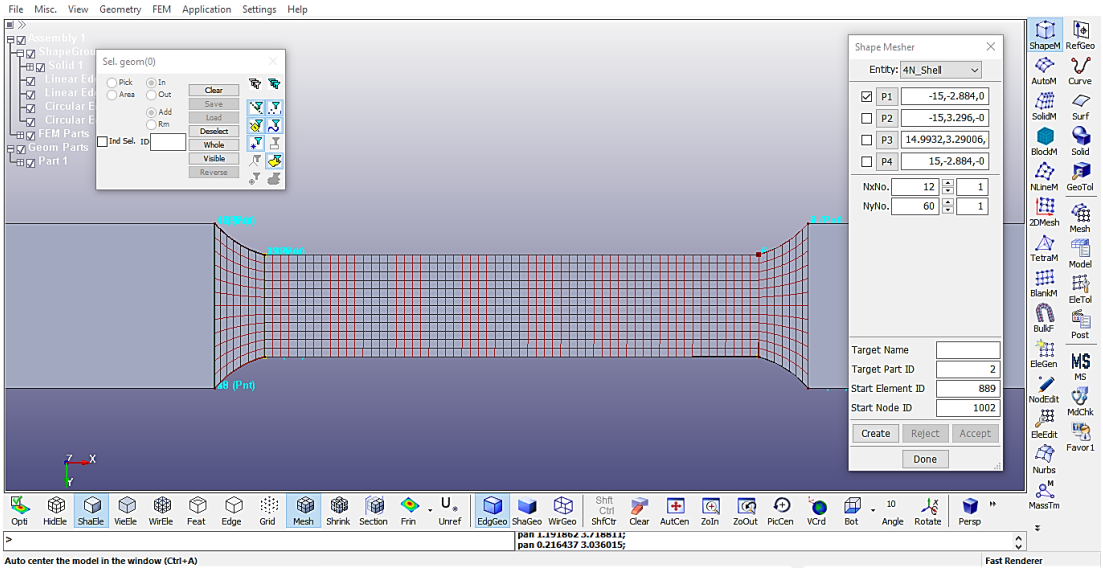

Figure 2: Meshing by using Shape Mesh

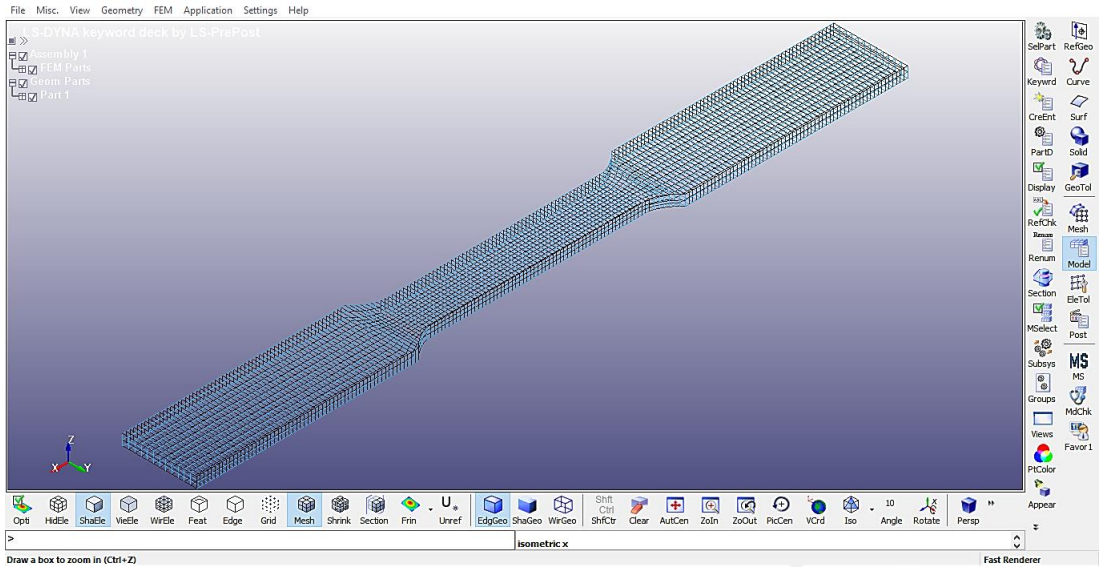

Figure 3: Meshed geometry of dog bone specimen

2.3 Boundary conditions

Boundary conditions are constraints necessary for the solution of a boundary value. In this research, boundary conditions are set on both sides of the specimen, so that it become either fixed nodes or moving nodes. The boundary conditions are set that way because it is assumed that the specimen is being clamp during the pulling process is occur, so the specimen position that has been set will not moving. Figure 4 shows that the setting of boundary SPC and Prescribed Motion to determine the nodes that will be fix and move.

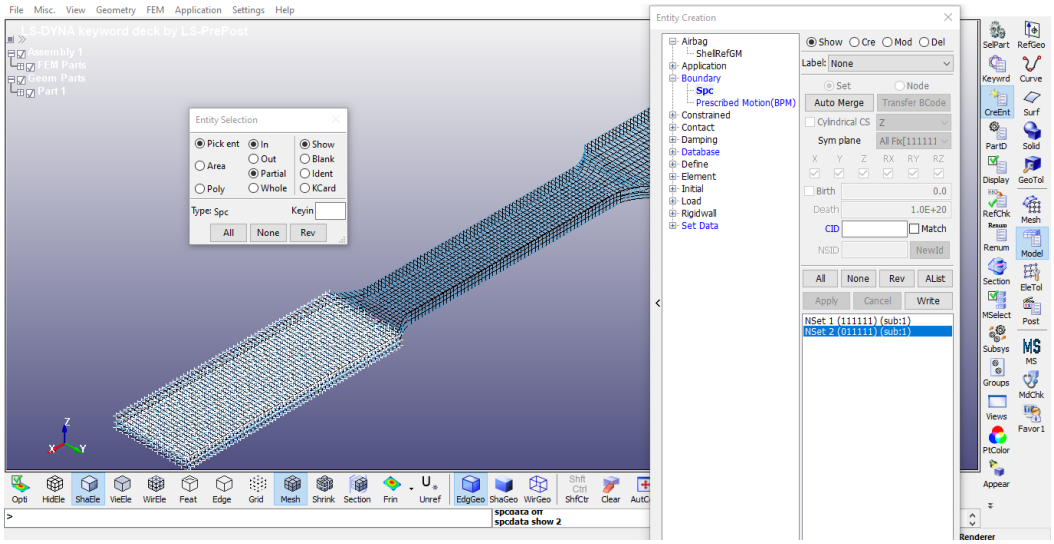

Figure 4: The setting of boundary SPC and Prescribed Motion

2.4 Simplified Johnson-Cook Characterisation

This study deals with the characterisation of DP 590 based on the simplified Johnson-Cook model which a strain and strain-rate dependent plasticity model requires the definition of four constants. The material's yield stress is represented by the constant A. The constant B allows for the strain hardening effect to be considered.

Simplified Johnson-Cook model is simplified from the original Johnson-Cook model which does not account for the temperature effect. The flow stress model is expressed as:

$$\sigma_{eq} = [A + B\varepsilon^{n}][1 + C\ ln\dot{\varepsilon}^{*}] \quad (1)$$

Where σ is the equivalent stress, and ε is the equivalent plastic strain. The material constants are A, B, n and C. A is the yield stress of the material which in this work already obtained from previous experiment as listed in Table 2. B is the strain hardening constant, n is the strain hardening coefficient and C is the strengthening coefficient of strain rate [10].

For determination of constant B and n, the deformation strain rate is $\dot{\varepsilon} = \dot{\varepsilon}_{ref} = 1s^{-1}$, equation (1) modified as follows:

$$\sigma = [A + B\varepsilon^{n}] \quad (2)$$

By rearranging Equation (2) and taking the natural logarithm on both sides, the modified equation can be obtained as shown below:

$$\ln(\sigma - A) = n\ ln\varepsilon + \ln B \quad (3)$$

By substituting the flow stress and strain values at the reference deformation conditions into Equation (3), the linear relationship plot between $\ln(\sigma - A)$ and $ln\varepsilon$ was drawn as depicted in Figure 5, and then the first-order regression model was used to fit the data points, it should be observed that the data is extremely close to the regression line, indicating that the data distribution is more predictable. As a result, the material constants B and n from the slope and intercept of the fitted curve.

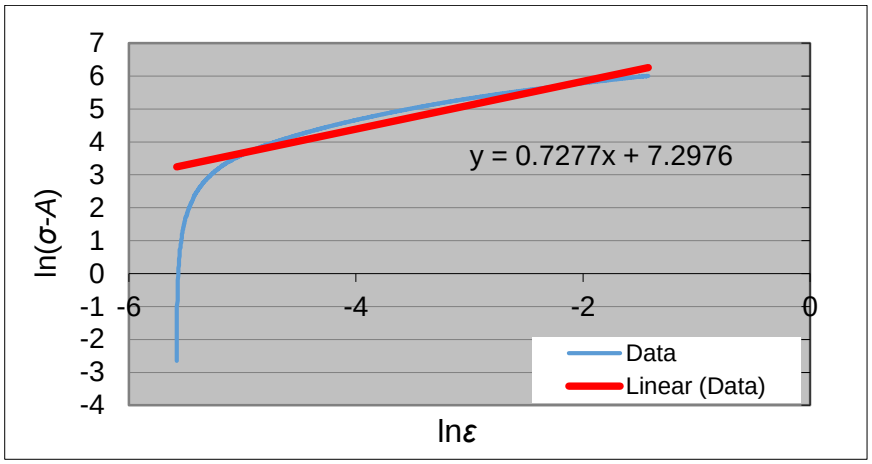

Figure 5: Relationship between $\ln(\sigma - A)$ and $ln\varepsilon$ under the reference conditions

After the parameters A, B and n were defined, determine the material constant C, by rearranging Equation (1) will result in the following form:

$$\frac{\sigma}{(A+B\varepsilon^{n})} = (1 + C\ ln\dot{\varepsilon}^{*}) \tag{4}$$

Initially, the values of material constants A, B and n, that have been obtained, were substituted into Equation (4); then, $\frac{\sigma}{(A+B\varepsilon^{n})} \sim ln\dot{\varepsilon}^{*}$ was drawn as a curve as shown in Figure. Following that, linear fitting was performed using a first-order regression model with a 1 as the intercept value, considering flow stress values at four strain rates (0.0001, 0.001, 0.01 and 0.1 s/1). Finally, the slope of the fitting curve, the material constant value, C, was estimated. The optimization approach was used in this study to determine the ideal C value in order to lower the prediction error when compared to experimental data. After that, the estimated values were employed in a numerical analysis to validate the parameters.

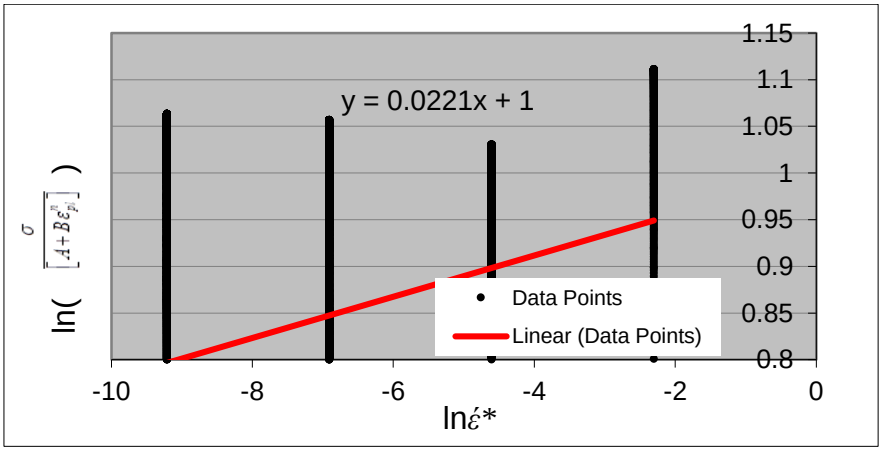

Figure 6: Relationship between $\frac{\sigma}{(A+B\varepsilon^{n})}$ and $ln\dot{\varepsilon}^{*}$

3. Results and Discussion

Tensile test has been simulated using LS Dyna finite element analysis to validate the characterised parameters and to analysis the comparison of stress-strain curve at various strain rates with the experimental test results. Among the several material models that are available, simplified Johnson-Cook model, known as MAT_098 in LS Dyna, has been selected for quasi-static strain rate to analyse the simulation.

The results obtained for each crosshead speed directed to longitudinal and transverse with different strain rates were compared to experimental results. The stress-strain curves of the analysed patterns in an elastoplastic stage are shown in Figure 7 to Figure 10.

As we can see the stress-strain curve illustrated in Figure 7 to Figure 10 by the simulations and experiments below, the results obtained are very close between the simulations and the experiments. In addition, the strain rate effect is not significant and it is actually consistent with the small value of the constant C. Besides the curves extracted from the simulation are smooth. The transition between the elastic and plastic regions is also smooth. For this range of strain rate, the simplified Johnson-Cook model seems to give slightly accurate results.

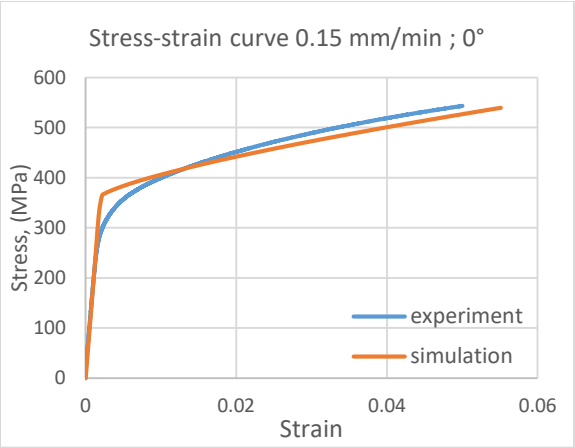

(a)

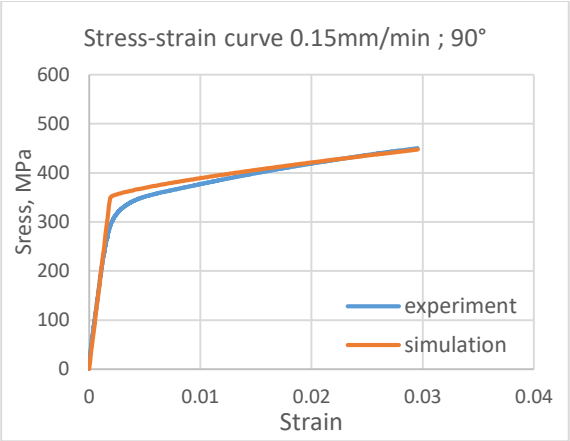

(b)

Figure 7: Comparison stress-strain curve for cross head speed 0.15 mm/min between experiment and simulation. (a) longitudinal (b) transverse

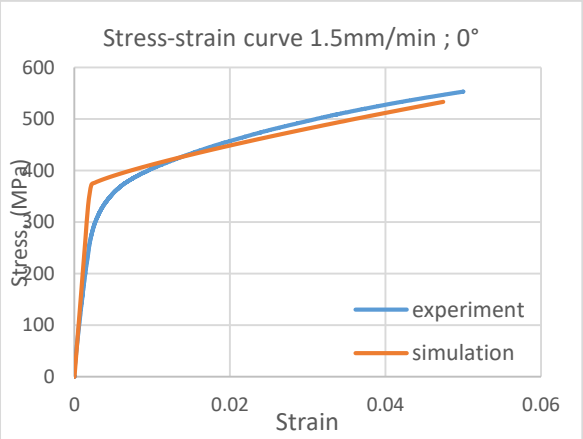

(a)

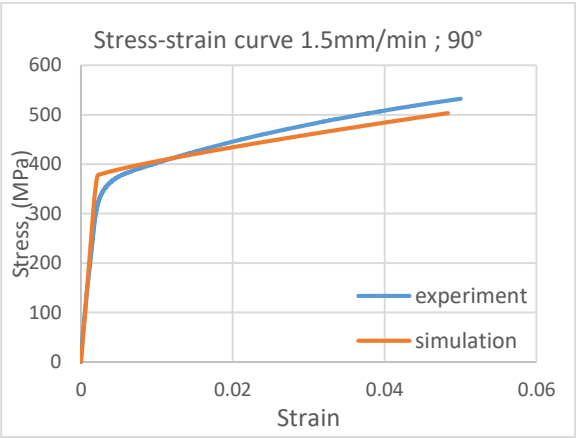

(b)

Figure 8: Comparison stress-strain curve for cross head speed 1.5 mm/min between experiment and simulation. (a) longitudinal (b) transverse

Research Progress in Mechanical and Manufacturing Engineering Vol. 2 No. 2 (2021) 380-389

RPMME

Homepage: http://publisher.uthm.edu.my/periodicals/index.php/rpmme
e-ISSN : 2773-4765

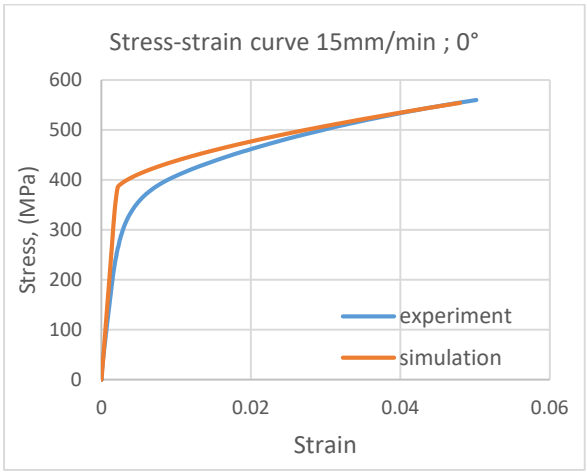

(a)

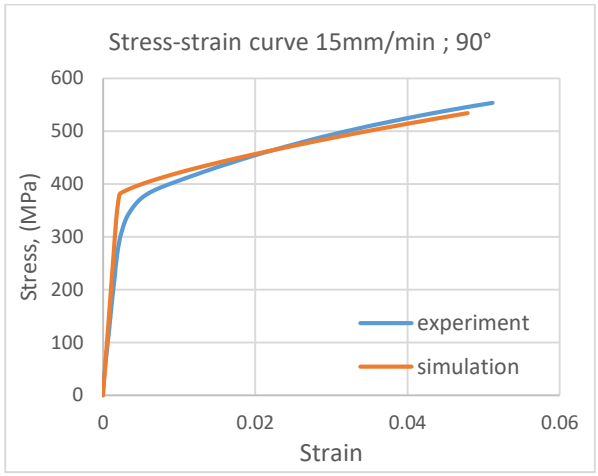

(b)

Figure 9: Comparison stress-strain curve for cross head speed 15 mm/min between experiment and simulation. (a) longitudinal (b) transverse

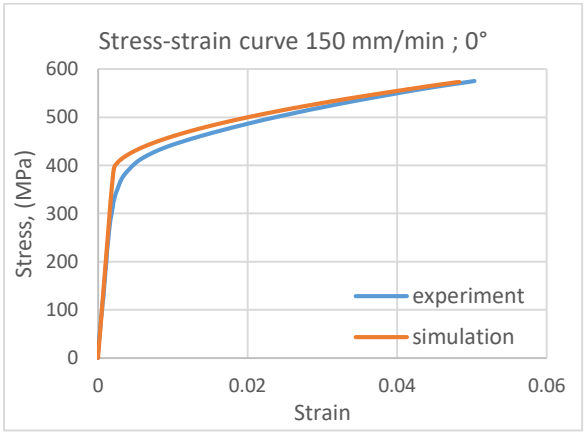

(a)

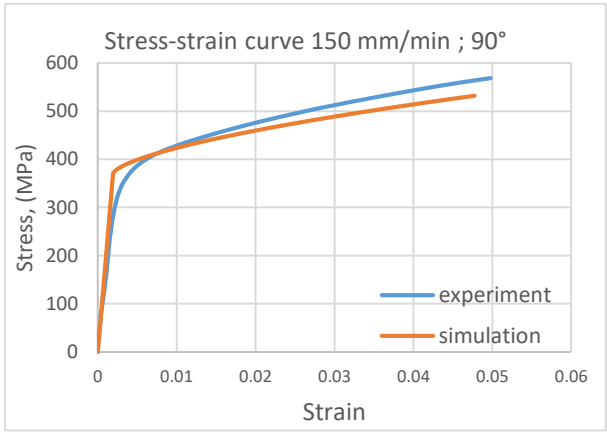

(b)

Figure 10: Comparison stress-strain curve for cross head speed 150 mm/min between experiment and simulation. (a) longitudinal (b) transverse

3.1 Comparison of stress-strain curve in longitudinal and transverse directions

The deformation behaviour of DP 590 subjected to various strain rates is discussed in this section in terms of stress-strain curves. These analyses are particularly relevant for DP steel deformation because stress-strain curves are a graphical representation of a material's mechanical characteristics that is heavily influenced by changes in strain rates. The stress-strain curves in the longitudinal and transverse directions are shown in Figures 11 and 12.

Generally, it can be clearly seen from these figures that the specimen exhibits strain rates sensitivity. Other than that, it can be observed that the proposed constitutive model which is the simplified Johnson-Cook, shows a good agreement with the strain rate sensitivity of the specimen using the proposed approach. It is observed that flow stress correlates with the strain rate. To be concluded, increasing the strain rate will increases the flow stress. In term of direction of material, this behaviour can be clearly observed that the longitudinal direction (rolling) has better mechanical properties compared to the

*Corresponding author: *khir@uthm.edu.my*

transverse direction. The flow stress is also higher in the longitudinal direction compared to transverse direction, and consistent in all strain rates.

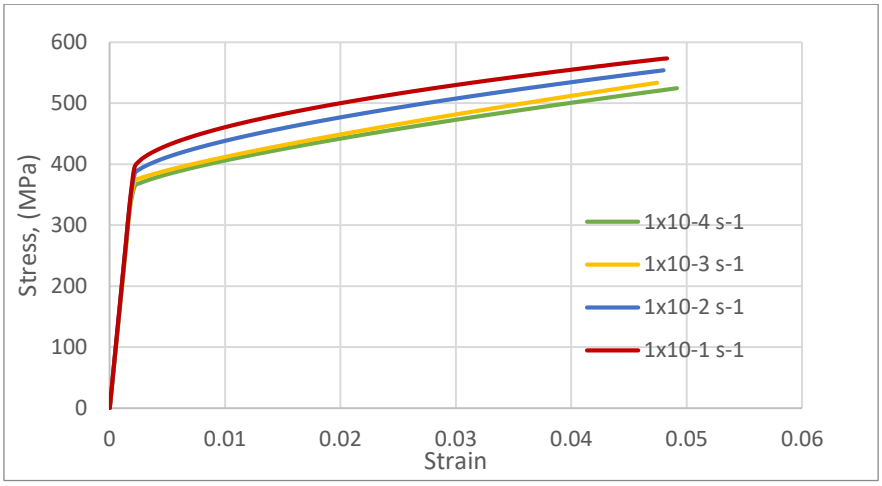

Figure 11: stress strain curve in longitudinal direction

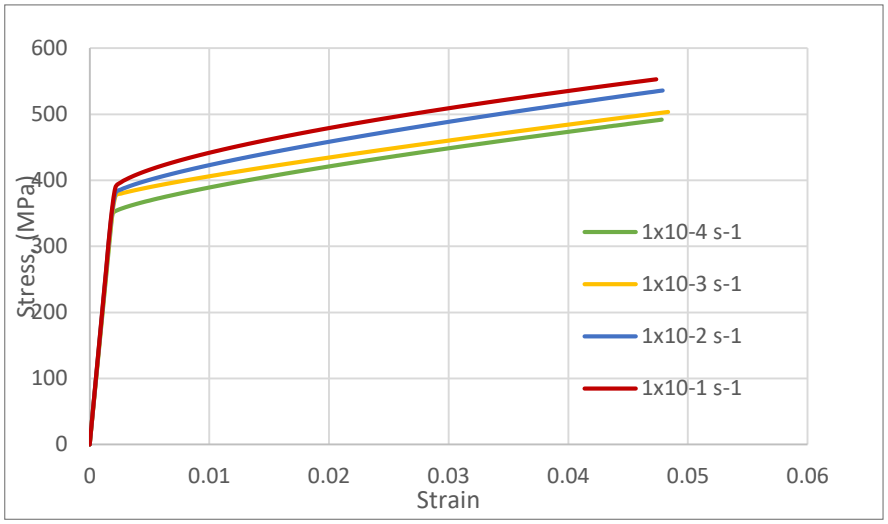

Figure 12: stress strain curve in transverse direction

4. Conclusion

In this research, the simulation of four different strain rates subjected to dog bone shape specimen of DP 590 steel have been conducted. The engineering data obtained from the previous experiment was characterised to define the parameters of DP 590 steel by using the simplified Johnson-Cook material model. The deformation behaviour of DP 590 steel also had been analysed in term stress-strain curve within the elastoplastic region of the deformed specimen. The numerical analysis performed using solid element of LS Dyna showed a good agreement at each strain rates.

Acknowledgement

Authors wish to convey a sincere gratitude to the Ministry of Higher Education (MOHE) for providing the financial means during the preparation to complete this research under Fundamental Research Grant Scheme (FRGS) – FRGS/1/2020/TK02/UTHM/02/5, Vot K331, and UTHM Contract Research Grant – Vot H276, respectively.

References

[1] R. Kuziak, R. Kawalla, and S. Waengler, "Advanced high strength steels for automotive industry: A review," *Arch. Civ. Mech. Eng.*, vol. 8, no. 2, pp. 103–117, 2008, doi: 10.1016/s1644-9665(12)60197-6.

[2] S. Pandre, P. Takalkar, N. Kotkunde, S. K. Singh, and A. Ul Haq, "Influence of temperatures and strain rates on tensile deformation behaviour of DP 590 steel," *Mater. Today Proc.*, vol. 18, pp. 2603–2610, 2019, doi: 10.1016/j.matpr.2019.07.119.

[3] J. Zhao and Z. Jiang, "Thermomechanical processing of advanced high strength steels," *Prog. Mater. Sci.*, vol. 94, no. January, pp. 174–242, 2018, doi: 10.1016/j.pmatsci.2018.01.006.

[4] M. Murugesan and D. W. Jung, "Johnson cook material and failure model parameters estimation of AISI-1045 medium carbon steel for metal forming applications," *Materials (Basel).*, vol. 12, no. 4, 2019, doi: 10.3390/ma12040609.

[5] A. Nasser, A. Yadav, P. Pathak, and T. Altan, "Determination of the flow stress of five AHSS sheet materials (DP 600, DP 780, DP 780-CR, DP 780-HY and TRIP 780) using the uniaxial tensile and the biaxial Viscous Pressure Bulge (VPB) tests," *J. Mater. Process. Technol.*, vol. 210, no. 3, pp. 429–436, 2010, doi: 10.1016/j.jmatprotec.2009.10.003.

[6] S. Curtze, V. T. Kuokkala, M. Hokka, and P. Peura, "Deformation behavior of TRIP and DP steels in tension at different temperatures over a wide range of strain rates," *Mater. Sci. Eng. A*, vol. 507, no. 1–2, pp. 124–131, 2009, doi: 10.1016/j.msea.2008.11.050.

[7] Y. Cao, B. Karlsson, and J. Ahlström, "Temperature and strain rate effects on the mechanical behavior of dual phase steel," *Mater. Sci. Eng. A*, vol. 636, pp. 124–132, 2015, doi: 10.1016/j.msea.2015.03.019.

[8] S. K. Paul, "Real microstructure based micromechanical model to simulate microstructural level deformation behavior and failure initiation in DP 590 steel," *Mater. Des.*, vol. 44, pp. 397–406, 2013, doi: 10.1016/j.matdes.2012.08.023.

[9] V. Panov, "Modelling of Behaviour of Metals at High Strain Rates," *Ph.D. Thesis*, p. 209, 2006.

[10] M. Murugesan and D. W. Jung, "Johnson cook material and failure model parameters estimation of AISI-1045 medium carbon steel for metal forming applications," *Materials (Basel).*, vol. 12, no. 4, 2019, doi: 10.3390/ma12040609.